Environmentally Assisted Cracking of Alloy 7050-T7451 Exposed to Aqueous Chloride Solutions

REINHOLD BRAUN

The stress corrosion cracking (SCC) behavior of 7050-T7451 plate material was investigated in short-transverse direction performing constant load and constant extension rate tests. Smooth and notched tensile specimens were permanently immersed in substitute ocean water and in an aqueous solution of 0.6 M NaCl + 0.06 M $(NH_4)_2SO_4$. Alloy 7050-T7451 exhibited high SCC resistance in both synthetic environments. However, conducting cyclic loading tests, environment-induced cracking was observed. Applying a sawtooth waveform, notched tensile specimens were strained under constant load amplitude conditions at constant displacement rates ranging from 2×10^{-6} to 2×10^{-4} mms^{-1}. The stress ratio $R = \sigma_{min}/\sigma_{max}$ was 0.1 with maximum stresses of 300 and 400 MPa. When cyclically loaded in substitute ocean water, notched specimens failed predominantly by transgranular environment-induced cracking. Striations were observed on the cleavage-like facets. The number of cycles-to-failure decreased with decreasing displacement rate. A slope of 0.5 was obtained by fitting the logarithmic plot of number of cycles-to-failure *vs* nominal loading frequency, indicating a hydrogen embrittlement mechanism controlled by diffusion.

DOI: 10.1007/s11661-015-3311-8

I. INTRODUCTION

HEAT-TREATABLE Al-Zn-Mg-Cu alloys are quite sensitive to stress corrosion cracking (SCC) in the peak strength T6 temper.[1–4] The SCC susceptibility, mostly pronounced when load is applied in the short-transverse direction, decreases from underaged to overaged microstructures. Using two-stage heat treatment practices, the resistance to stress corrosion cracking as well as exfoliation corrosion can be improved by overaging to various tempers, such as T76, T74, and T73, however, in general at the expense of strength (with sacrifices from 5 to 20 pct).[5–7] The patented T77 temper is the only heat treatment which provides good exfoliation corrosion behavior and SCC resistance superior to that of the T6 temper without concomitant loss in strength.[6,7] Environment-induced failure in service has not occurred with Al-Zn-Mg-Cu alloys in the overaged T73 heat treatment.[3,7] Similarly, no instances of SCC failure have been reported for alloy 7050-T74, although SCC laboratory tests can indicate sensitivity to stress corrosion cracking when severe testing conditions are applied.[7] The latter alloy was developed to provide high strength in thick section products, adequate fracture toughness, and fatigue characteristics as well as high exfoliation corrosion and stress corrosion cracking resistances.[6]

Stress corrosion cracking causing failure in commercial aluminum alloys is generally intergranular and promoted by water-containing environments.[1–4] The growth of cracks is accelerated by the presence of chloride which is found everywhere in marine or rural atmosphere. For aluminum alloys, two basic theories for SCC are proposed: cracking caused by anodic dissolution and hydrogen embrittlement.[8] However, the precise mechanisms promoting stress corrosion cracking in a sensitive alloy exposed to a particular environment still remain unclear. The prevailing SCC mechanism working in 2XXX and 5XXX aluminum alloys is generally considered intergranular corrosion accelerated and localized by the applied stress and controlled by the potential difference between grain and grain boundaries.[1,9] For Al-Zn-Mg alloys, hydrogen embrittlement is the dominant environment-induced failure mechanism, whereas both anodic dissolution and hydrogen embrittlement are considered being operative in 7XXX series alloys containing higher copper contents.[9–11] The accumulation of hydrogen in the plastic zone ahead the crack tip due to an increased hydrogen solubility in the plastically deformed area can induce intergranular decohesion resulting in crack advance by a hydrogen embrittlement mechanism.[12] The heat treatments developed to improve the SCC resistance are focused on the elimination of the susceptibility to intergranular stress corrosion cracking.[3] Even though stress corrosion cracks mainly propagate intergranularly in aluminum alloys, transgranular environmentally assisted cracking was also observed, particularly in 7XXX series alloys in overaged tempers.[3,4,13–16] Transgranular SCC occurred when severe loading conditions were applied. As supported by fractography and metallography, transgranular stress corrosion cracks initiated very often from pitting corrosion attacks, acting as stress raiser. This environment-induced cleavage-like fracture showed

REINHOLD BRAUN, Senior Research Engineer, is with the Institute of Materials Research, DLR German Aerospace Center, 51170 Köln, Germany. Contact e-mail: reinhold.braun@dlr.de
Manuscript submitted May 13, 2015.
Article published online January 6, 2016

crystallographic parallel facets separated by steps, frequently exhibiting fan-like pattern. Crack-arrest markings on the fracture surface indicated discontinuous crack propagation.

Generally, the SCC behavior of a material is evaluated determining threshold stresses σ_{th} and K_{ISCC} below which stress corrosion cracking is not assumed to occur.[2,17] To measure these SCC threshold stresses, tests are carried out under static or monotonic loading conditions, as applied in constant load, constant strain, and slow strain rate tests using smooth or pre-cracked specimens.[18] However, superposition of a cyclic load with small amplitude upon a larger static load, so-called "ripple" loading, can significantly decrease the SCC resistance of rather immune alloys.[19] Performing cyclic loading tests with a stress ratio of $R = 0.9$ in an aqueous 3.5 pct NaCl solution, cracking was induced in alloy 7075-T7351 at stress intensity factors being up to 60 pct lower than the K_{ISCC} value determined using the slow strain rate testing technique.[20] Investigating the interface between stress corrosion cracking and corrosion fatigue, the conditions for SCC propagation in mild steel immersed in carbonate-bicarbonate solution were found to be maintained by cyclic loading at significantly lower stress intensity levels where stress corrosion cracking did not occur under static loading.[21] For α-brass immersed in sodium nitride solution, continuing micro-plastic deformation was required to initiate environment sensitive cracking.[22] Under cyclic loading conditions, such plastic deformation is induced at lower stresses in comparison to monotonic loading, thus reducing the threshold stresses for cracking. The loading frequency might affect the environmentally assisted crack velocity. As observed in corrosion fatigue tests of 7XXX series aluminum alloys using aqueous chloride-containing solutions, the crack propagation rate increased with decreasing frequency.[23,24] For alloy 7050-T7651, the number of cycles-to-failure was found to decrease with deceasing frequency performing cyclic loading tests in substitute ocean water at applied maximum stress which was below the threshold stress observed in static loading tests.[15] Failure was caused by transgranular environment-induced cracking. Similar results were obtained from SCC tests of 7475 plate material.[14] When statically loaded at applied stresses up to 600 MPa, short-transverse-oriented notched tension specimens of 7475-T7351 did not fail during the maximum exposure length of 1000 hours in substitute ocean water. However, when notched specimens were cyclically loaded at an average stress of 500 MPa with stress amplitude of ±100 MPa, failure was observed after 290 hours, corresponding to 300 cycles at the applied displacement rate of 3.2×10^{-5} mms^{-1}.

Besides loading conditions, the environment plays an important role inducing environmentally assisted cracking. Therefore, the corrosive media used in accelerated laboratory corrosion tests should be relevant to service conditions. In addition to chlorides, industrial environments can contain nonhalide pollutants, such as sulfates and nitrates.[25,26] To simulate corrosion in inland polluted environments, a mixture of sodium chloride and ammonium sulfate was found to be an appropriate synthetic environment.[25] The various anions often show a synergistic effect on stress corrosion cracking.[27–30] Whereas pure NaCl solutions did not promote SCC in 2XXX and 7XXX series aluminum alloys under permanent immersion conditions, the additions of sulfate, nitrate, bicarbonate, or hydrogen phosphate were found to induce cracking.[28,29] This was probably associated with inhibiting effects of these anions, keeping the crack sharp by passivation of the crack walls. The aim of the present work was to study the environmentally assisted cracking behavior of the overaged alloy 7050-T7451 in short-transverse direction using different synthetic environments and loading conditions.

II. EXPERIMENTAL

The material used was a 45-mm-thick plate of the alloy 7050 in the temper T7451. Short-transverse tensile properties of the 7050-T7451 plate, determined by tensile testing of quintuplicate samples, were as follows: 0.2 pct yield strength = 446 ± 5 MPa, ultimate tensile strength = 532 ± 1 MPa, and fracture elongation = 8.1 ± 0.7 pct. From this plate, smooth and notched round tension specimens were machined in short-transverse orientation. The smooth specimens had a gage length of 15.7 mm and a cross section of 10 mm^2. In the center of the gage length of the notched specimens, a 60 deg circumferential V-notch was machined with a depth of 0.61 mm and a notch tip radius of 0.14 mm. The root diameter was 3.50 mm. The notch strength of the 7050-T7451 specimens related to the specified sample geometry was determined to 677 ± 14 MPa.

The SCC behavior of the 7050-T7451 plate was investigated performing constant load tests and constant extension rate tests. Smooth and notched tension specimens were permanently immersed in (i) substitute ocean water without heavy metals (ASTM D1141) and (ii) an aqueous solution of 0.6 M NaCl + 0.06 M $(NH_4)_2SO_4$ at free corrosion potential. The synthetic environments were prepared immediately prior to use and thoroughly aerated. Constant load tests were carried out using dead weight loaded tensile testing machines. Maximum exposure time periods were 1000 and 2000 hours for smooth and notched specimens, respectively. Failure criterion was fracture. Constant extension rate testing (CERT) was performed applying cross-head displacement rates ranging from 2×10^{-6} to 3×10^{-5} mms^{-1}. Fracture energy, determined by the area beneath the stress-*vs*-strain curve, and notch strength were used to evaluate sensitivity to environmentally assisted cracking when straining smooth and notched tension specimens, respectively. Reference tests were carried out in dry laboratory air (inert environment) generated by embedding the specimens in magnesium perchlorate hydrate (~83 pct $Mg[ClO_4]_2$) powder. Pre-exposure tests were performed to determine the degradation of specimens caused by immersion in the corrosive environment in the absence of an applied stress. Unstressed specimens were immersed in the synthetic environment for exposure periods corresponding to the immersion times during the constant extension

rate tests. After pre-exposure, the samples were dynamically strained in an inert environment at the same extension rates as in the corrosive environment. Details of the CERT technique are described elsewhere.[31]

The environmentally assisted cracking behavior was also studied under cyclic loading conditions using notched tension specimens which were permanently immersed in aerated substitute ocean water at free corrosion potential. These tests were carried out under constant load amplitude at constant cross-head speed employing a slow strain rate testing machine. A saw-tooth-shaped waveform was used; the load increased from a lower to an upper fixed value. The displacement rates were in the range from 2×10^{-6} to 2×10^{-4} mms^{-1}. The maximum load levels applied corresponded to maximum stresses σ_{max} of 300 and 400 MPa with regard to the original cross-sectional area at the notch. The stress ratio $R = \sigma_{min}/\sigma_{max}$ was 0.1 for all tests. Depending upon the displacement rate and load levels, the resulting nominal frequencies ranged from 10^{-5} to 10^{-3} s^{-1}, calculated by dividing the number of cycles-to-failure by the time-to-failure. The loading frequency might vary during testing due to cyclic hardening and softening of the aluminum alloy samples. Whereas pronounced cyclic hardening effects were observed for underaged Al-Zn-Mg-(Cu) alloys, their microstructure remained quite stable during cycling in the peak-aged temper.[32] This is also supposed for the overaged alloy 7050-T7451 used, and, therefore, the frequency is not expected to vary significantly during cyclic loading testing carried out in this work.

Before testing, the specimens were ultrasonically cleaned in ethanol and degreased in acetone vapor. Fracture surfaces were examined by scanning electron microscopy (SEM) after cleaning using an aqueous solution of chromic and phosphoric acids, as recommended in ASTM Standard Practice G1 for aluminum alloys.

III. RESULTS

Constant load tests indicated high short-transverse SCC resistance of alloy 7050-T7451 when exposed to substitute ocean water and an aqueous solution of 0.6 M NaCl + 0.06 M $(NH_4)_2SO_4$ (Table I). Smooth and notched tensile specimens did not fail during 1000 and 2000 hours, respectively, at an applied stress of 400 MPa. This was corroborated by measurements of the residual strength after exposure. For smooth specimens, residual strengths between 527 and 530 MPa were obtained, corresponding to the ultimate tensile strength of the 7050-T7451 plate. The fracture surfaces of these specimens revealed a completely ductile dimple-like fracture.

Results of the constant extension rate tests are presented in Figure 1, using smooth tension specimens. At the displacement rates applied, the fracture energy values were quite similar for specimens dynamically strained in the corrosive media and an inert environment. As confirmed by pre-exposure tests, the slight decrease in fracture energy for the samples tested in the aggressive environments at lower displacement rates was mainly caused by corrosion processes independent of stress, like pitting and intergranular corrosion.

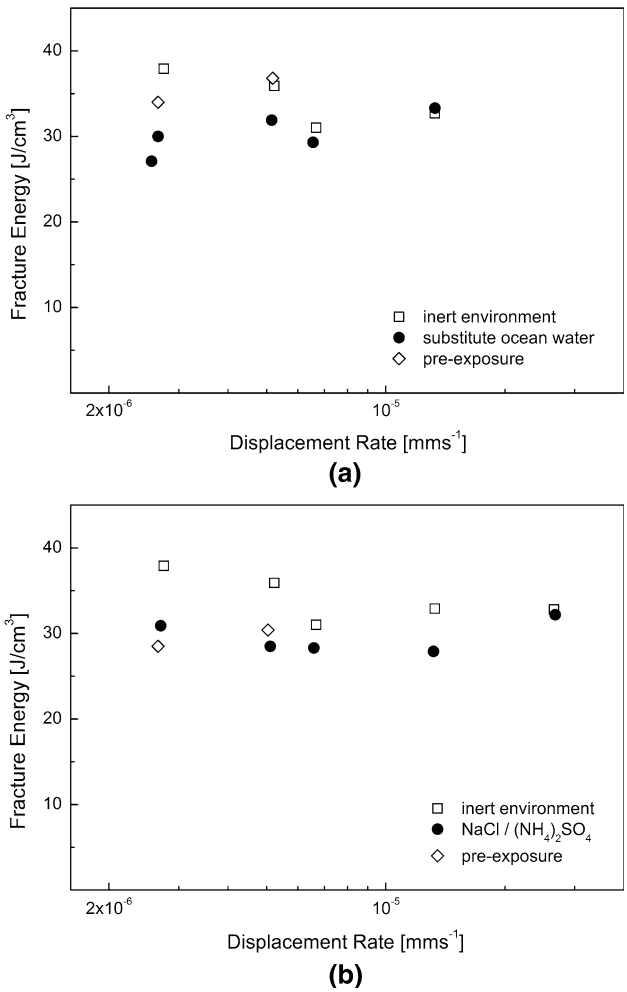

Fig. 1—Curves of fracture energy *vs* displacement rate for alloy 7050-T7451 plate. Smooth short-transverse tensile specimens were dynamically strained in an inert environment as well as in (*a*) substitute ocean water and (*b*) an aqueous solution of 0.6 M NaCl + 0.06 M $(NH_4)_2SO_4$. Data for pre-exposed specimens are included.

Table I. Time-To-Failure Data of Alloy 7050-T7451 Plate Obtained from Constant Load Tests

Electrolyte	Smooth Tensile Specimens (h)	Notched Tensile Specimens (h)
Substitute ocean water	>1000	>2000
0.6 M NaCl + 0.06 M $(NH_4)_2SO_4$	>1000	>2000

Triplicate smooth and notched tensile specimens were permanently immersed in substitute ocean water and an aqueous solution of 0.6 M NaCl + 0.06 M $(NH_4)_2SO_4$ at an applied stress of 400 MPa in short-transverse direction. None of the samples failed.

Figure 2 shows results of the CERT technique using notched tensile specimens. The notched strength is plotted for duplicate specimens which were dynamically strained in an inert environment, substitute ocean water, and an aqueous solution of 0.6 M NaCl + 0.06 M $(NH_4)_2SO_4$ at a displacement rate of 2×10^{-6} mms^{-1}. Considering the scatter band of ±14 MPa for the short-transverse notch strength (see section Experimental), similar values were obtained for samples strained under inert and aggressive environmental conditions (further scatter might be associated with corrosion attack during immersion in the corrosive environment, as corroborated by fractographic examinations revealing few areas of pitting corrosion). Thus, in accordance with constant load tests, the CERT technique indicated high SCC resistance of alloy 7050-T7451 when both smooth and notched tension specimens were used. Isolated transgranular SCC was observed at the rim of the fracture surfaces of smooth and notched specimens which were strained in substitute ocean water at a displacement rate of 2×10^{-6} mms^{-1} (Figure 3). This type of environmentally assisted cracking was not observed with specimens immersed in an aqueous chloride-sulfate solution. However, transgranular SCC did not substantially degrade the fracture energy and notch strength determined for specimens strained in substitute ocean water, probably occurring at high stresses applied just before fracture.

Results of the cyclic loading tests are listed in Table II and are plotted in Figure 4. Applying stress ranges $\Delta\sigma = \sigma_{max} - \sigma_{min}$ of 360 and 270 MPa with σ_{max} of 400 and 300 MPa, respectively, notched short-transverse 7050-T7451 specimens were cyclically loaded at different displacements rates. All tests were carried out at an *R*-ratio of 0.1. The nominal loading frequency depended upon the stress range and displacement rate used. The time-to-failure decreased with increasing displacement rate (Figure 4(a)). Failure occurred at shorter time with higher maximum stress. The number of cycles-to-failure decreased with decreasing nominal frequency (Figure 4(b)). At a given nominal frequency, the number of cycles-to-failure was higher for lower stress range $\Delta\sigma$, *i.e.*, for lower maximum stress. A linear dependence was found between the log values. On a log–log basis, the dependences were described by log *Y* (number of cycles-to-failure) = 0.513 log X (frequency) + 4.554 and log $Y = 0.492 \log X + 4.200$ for the data obtained applying maximum stresses of 300 and 400 MPa, respectively. For both curves, a slope of about 0.5 was obtained.

Fractographic examinations of the cyclically loaded specimens revealed a brittle transgranular fracture. At lower frequencies, corresponding to longer exposure time periods, intergranular fracture was also observed (Figure 5(a)). On the flat facets, fine quite regularly spaced striations were found as well as coarse brittle striations consisting of deep slots (Figure 5(b)). With increasing frequency, brittle transgranular crack propagation was prevailing (Figure 6(a)). Striation spacing increased, as the crack propagated in the interior of the material due to the higher stress resulting from a reduced cross-sectional area. On grain boundaries, the crack might change the fracture plane and propagation direction (Figure 6(b)).

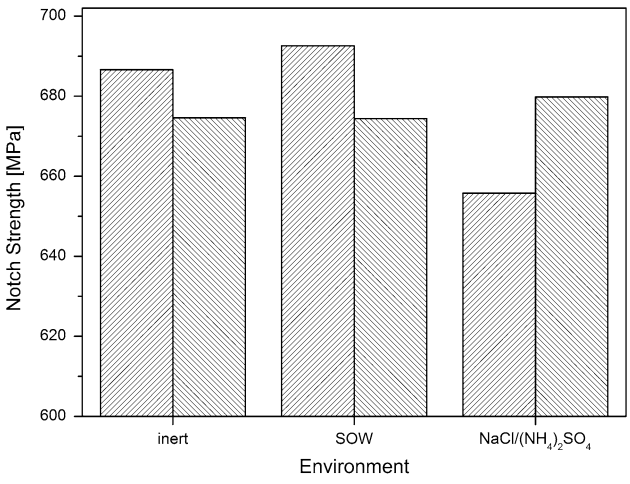

Fig. 2—Results of constant extension rate tests for alloy 7050-T7451 plate using notched short-transverse tensile specimens. Duplicate specimens were dynamically strained in an inert environment, substitute ocean water (SOW), and an aqueous solution of 0.6 M NaCl + 0.06 M $(NH_4)_2SO_4$ at a displacement rate of 2×10^{-6} mms^{-1}.

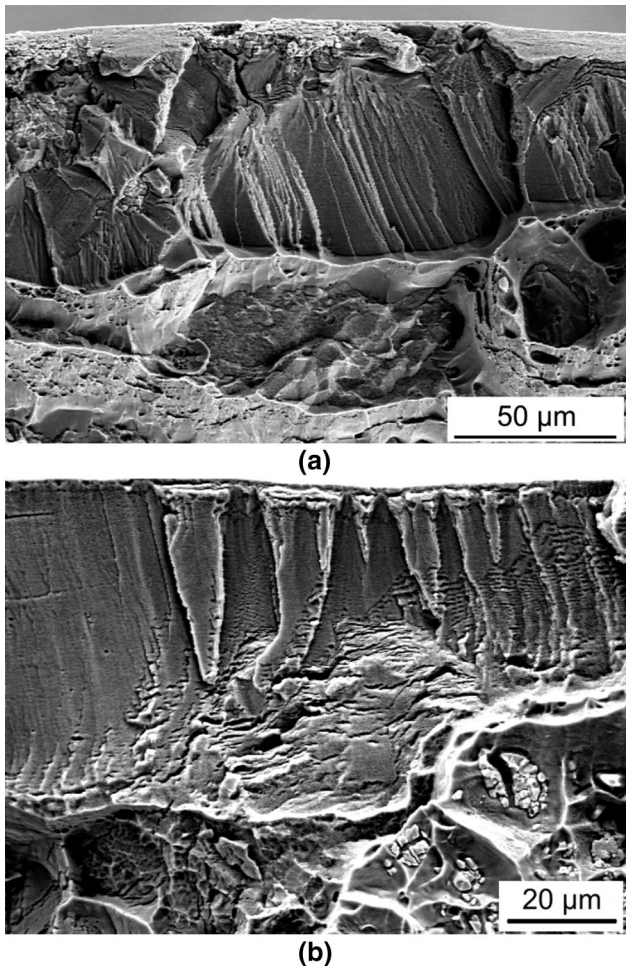

Fig. 3—Scanning electron micrographs of alloy 7050-T7451 showing transgranular stress corrosion cracking. Smooth (*a*) and notched (*b*) short-transverse tensile specimens were dynamically strained in substitute ocean water at a displacement rate of 2×10^{-6} mms^{-1}.

Table II. Time-To-Failure Data of Alloy 7050-T7451 Plate Obtained from Cyclic Loading Tests

Displacement rate (mms^{-1})	Nominal Loading Frequency (s^{-1})	Cycles-to-Failure	Time-to-Failure (h)
$\Delta\sigma$ = 360 MPa with σ_{max} = 400 MPa			
2.5×10^{-6}	1.08×10^{-5}	55	1412
4.9×10^{-6}	2.11×10^{-5}	84	1108
6.3×10^{-6}	2.75×10^{-5}	96	968
1.3×10^{-5}	5.42×10^{-5}	117	600
2.0×10^{-5}	8.55×10^{-5}	158	514
3.3×10^{-5}	1.41×10^{-4}	190	375
7.0×10^{-5}	3.10×10^{-4}	291	261
1.1×10^{-4}	4.70×10^{-4}	439	260
1.4×10^{-4}	6.11×10^{-4}	381	173
1.9×10^{-4}	7.91×10^{-4}	454	159
$\Delta\sigma$ = 270 MPa with σ_{max} = 300 MPa			
6.4×10^{-6}	3.61×10^{-5}	183	1409
2.0×10^{-5}	1.10×10^{-4}	337	855
3.3×10^{-5}	1.91×10^{-4}	491	715
1.1×10^{-4}	6.40×10^{-4}	781	339
1.9×10^{-4}	1.03×10^{-3}	1046	283

Notched short-transverse tensile specimens were tested in substitute ocean water at different displacement rates and stress ranges $\Delta\sigma = \sigma_{max} - \sigma_{min}$.

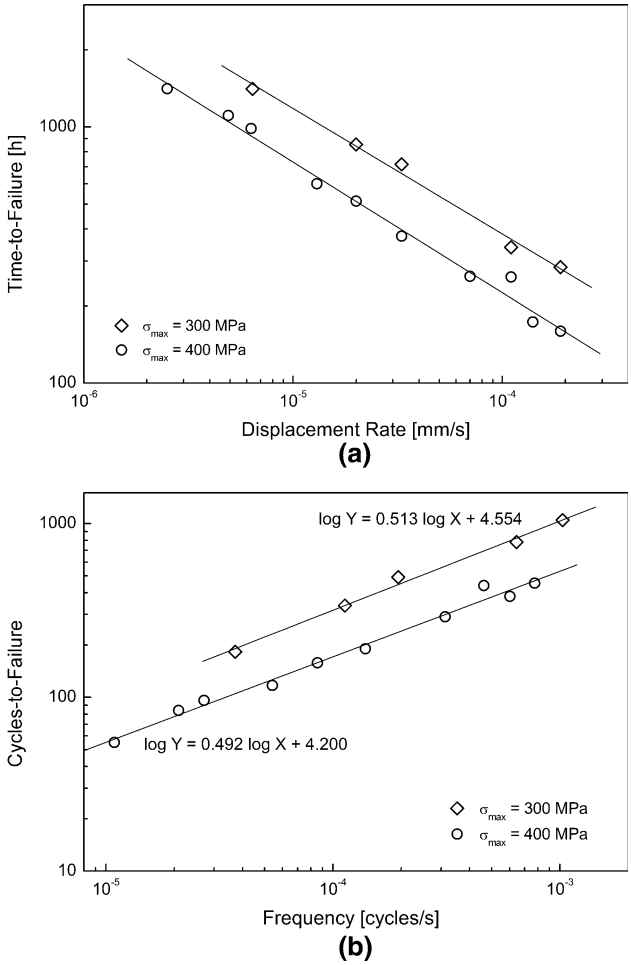

Fig. 4—Curves of (*a*) time-to-failure *vs* displacement rate and (*b*) number of cycles-to-failure *vs* nominal frequency for alloy 7050-T7451. Notched short-transverse specimens were cyclically loaded in substitute ocean water applying different maximum stresses at an R-ratio of 0.1. Results of linear fits on a log–log basis are included in the cycles-to-failure *vs* frequency plot.

Striations were found on cleavage-like facets as well as on intergranular environment-induced fracture planes, indicating discontinuous crack propagation for both transgranular and intergranular fracture modes (Figure 7). At higher frequencies up to 8×10^{-4} s^{-1}, the highest nominal frequency applied in this work, fine regularly spaced ductile striations predominately developed, probably indicating the crack advance per cycle, as shown in Figure 8 for a notched sample which was cyclically loaded at a nominal frequency of 6.11×10^{-4} s^{-1}. This type of striations is typically observed for 7XXX series aluminum alloys during fatigue crack propagation in air, resulting from extensive plastic blunting by shear at the crack tip.[33,34] Ductile striations were also present on fracture surfaces of high-strength aluminum alloy specimens fatigue tested in inhibited salt solutions,[33–35] and they formed, together with brittle striations, in salt solutions and water-vapor-containing environment.[36,37]

Similar fractographic features were observed for specimens cyclically loaded applying a stress range $\Delta\sigma$ of 270 MPa with a maximum stress of 300 MPa. At the lowest nominal frequency of 3.6×10^{-5} s^{-1}, environmentally assisted cracking was predominantly intergranular with cleavage-like fracture between two intergranular fracture planes (Figure 9). With increasing frequencies, a brittle transgranular fracture mode was prevalent with flat cleavage-like appearance (Figure 10). The nearly featureless facets revealed brittle striations with a roughened aspect. At even higher frequencies, fine ductile striations were observed again traversing several facets (Figure 11).

IV. DISCUSSION

The static loading tests carried out in the present work indicate high SCC resistance of alloy 7050-T7451 in short-transverse direction. No failure was observed for smooth and notched tensile specimens permanently

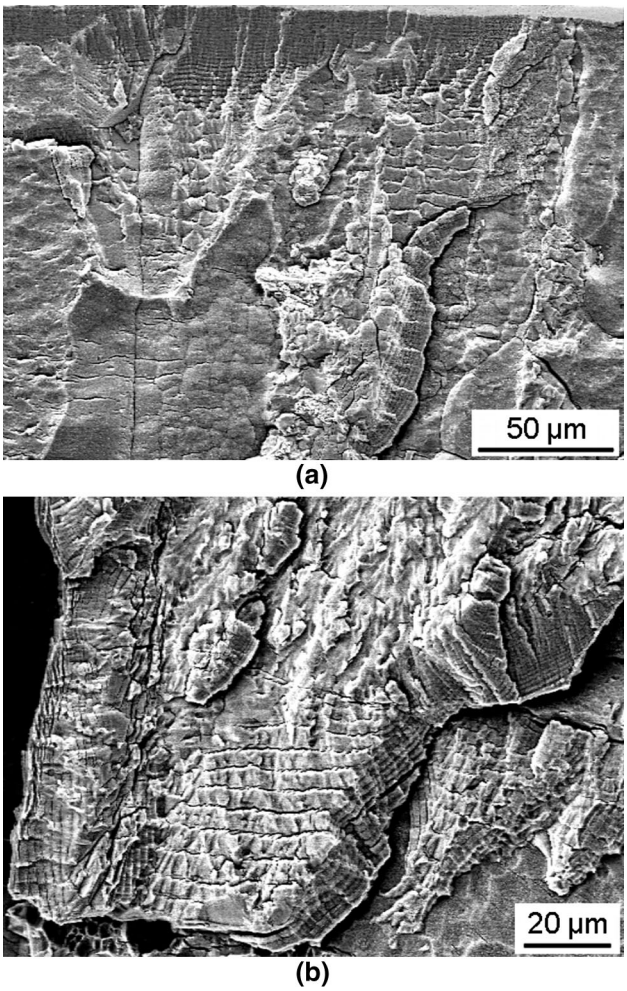

Fig. 5—Scanning electron micrographs of alloy 7050-T7451 showing (*a*) transition from transgranular to intergranular SCC and (*b*) fine and coarse striations on facets. The notched sample was cyclically loaded in substitute ocean water at a nominal frequency of 1.08×10^{-5} s^{-1}, applying a stress range $\Delta\sigma = 360$ MPa with $\sigma_{max} = 400$ MPa.

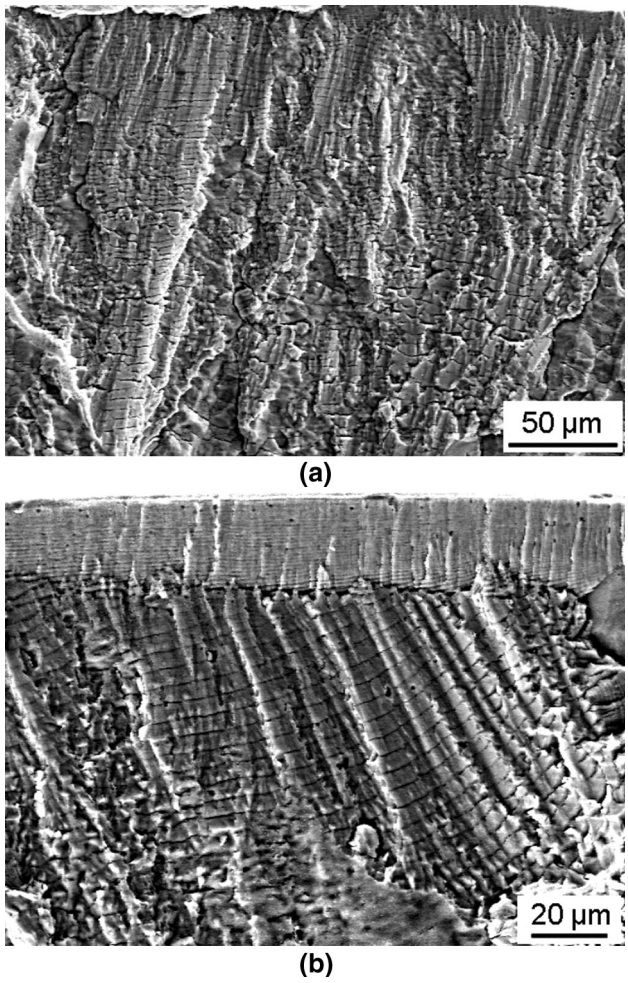

Fig. 6—Scanning electron micrographs of alloy 7050-T7451 showing (*a*) cleavage-like fracture and (*b*) crack propagation change between two cleavage-like facets. The notched sample was cyclically loaded in substitute ocean water at a nominal frequency of 2.11×10^{-5} s^{-1}, applying a stress range $\Delta\sigma = 360$ MPa with $\sigma_{max} = 400$ MPa.

immersed in aqueous chloride-containing solutions under constant load conditions at an applied stress of 400 MPa for exposure time periods exceeding 1000 h. This is in agreement with results of SCC tests reported in the literature. Minimum short-transverse SCC threshold stress determined by alternate immersion tests according to ASTM G44 for 480 hours (20 days) has been stated to be 240 MPa (35 ksi) for 25.2-mm-thick 7050-T7451 plate material.[6] A similar value of about 290 MPa was measured for alloy 7150-T7451 performing constant load tests under alternate immersion in aerated 3.5 pct NaCl solution for 720 hours (30 days).[9,13] Furthermore, for the high-strength Al-Zn-Mg-Cu alloy 7010 in the temper T7451, no sensitivity to environment-induced cracking in short-transverse direction was indicated by the slow stain rate testing technique using artificial sea water.[38] In the present study, intergranular SCC susceptibility was not detected by constant extension rate tests in substitute ocean water and an aqueous chloride-sulfate solution. When applied to evaluate the SCC behavior of aluminum alloys, the CERT technique was reported to be a useful tool to sort out quite sensitive alloys and to discriminate between alloys possessing low or high SCC resistance.[14,39–41] However, it failed to clearly indicate environmentally assisted cracking with moderately susceptible alloys. Dependent on the synthetic environments used, a large scatter in fracture energy data was observed for the latter alloys, or the degradation of the dynamically strained specimens was substantially caused by corrosion processes independent of stress, as revealed by pre-exposure tests. The assessment of SCC behavior is further hampered by considerable scatter in ductility often found for commercial semi-fabricated products of aluminum alloys tensile tested in corrosive as well as inert environments, in particular in short-transverse direction. Nevertheless, despite the limits of the applicability of the CERT technique, the results obtained in this work corroborate high SCC resistance of alloy 7050-T7451. Therefore, the overaged T74 heat treatment virtually provides

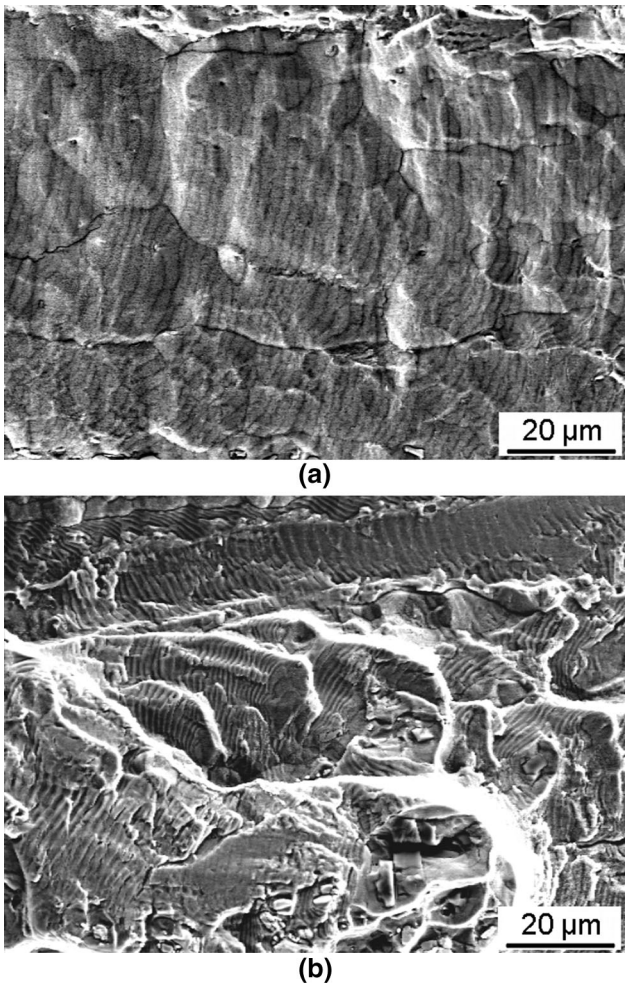

Fig. 7—Scanning electron micrographs of alloy 7050-T7451 showing striations on (*a*) intergranular fracture and (*b*) cleavage-like facets. The notched sample was cyclically loaded in substitute ocean water at a nominal frequency of 3.10×10^{-4} s^{-1}, applying a stress range $\Delta\sigma = 360$ MPa with $\sigma_{max} = 400$ MPa.

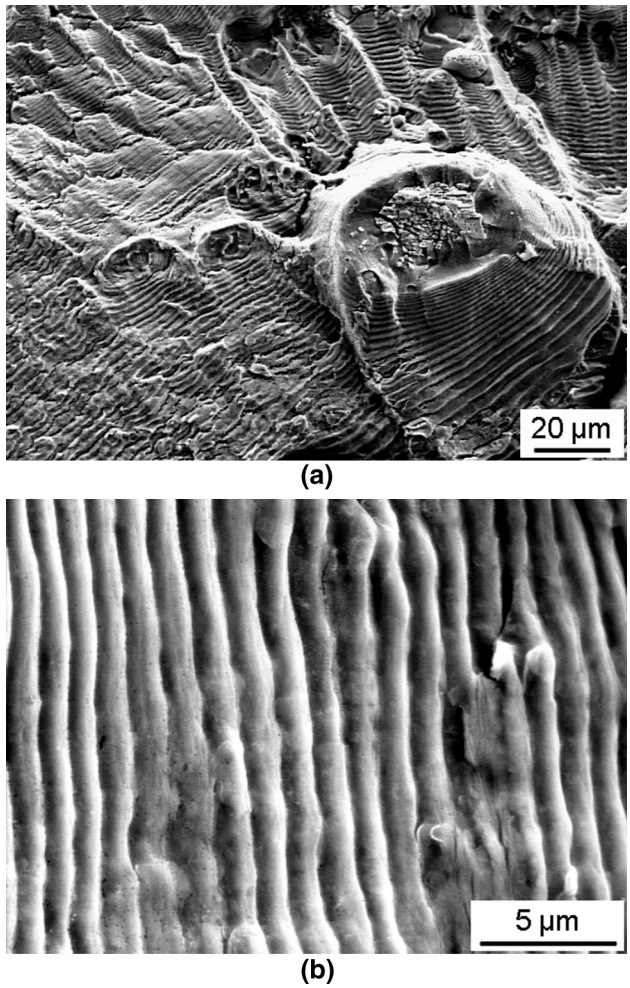

Fig. 8—Scanning electron micrographs of alloy 7050-T7451 showing striations (*a*) on cleavage-like facets and (*b*) on a facet indicating crack advance per cycle. The notched sample was cyclically loaded in substitute ocean water at a nominal frequency of 6.11×10^{-4} s^{-1}, applying a stress range $\Delta\sigma = 360$ MPa with $\sigma_{max} = 400$ MPa.

immunity to intergranular stress corrosion cracking. This is in accordance with the dependence of SCC sensitivity upon aging generally found with heat-treatable aluminum alloys that the SCC resistance increases from underaged to overaged tempers.[4,8]

However, transgranular stress corrosion cracking has been often observed for 7XXX series alloys in overaged tempers.[3,4,13,14,40–45] The fracture surfaces are characterized by cleavage-like facets with crystallographic orientation and river pattern as well as crack-arrest markings associated with discontinuous crack propagation.[46,47] This type of SCC also occurred in Al-Mg-Si and Al-Cu-Mg alloys under conditions of static loading at high stresses and dynamic straining to fracture at slow strain rates in chloride-containing environments.[40,48–50] Transgranular environment-induced cracks initiated very often from pitting corrosion attacks,[3,13,14] but they were also observed to propagate from smooth surfaces without localized corrosion attack.[51,52] For Al-Zn-Mg-Cu alloys in overaged tempers, transgranular stress corrosion cracking was promoted in aqueous chloride solutions containing nitrates. For alloy 7050-T7451, failure caused by transgranular environment-induced cracking was observed in constant load tests under permanent immersion condition in an aqueous NaCl-$NaNO_3$ solution at stresses down to 200 MPa.[16] In contrast, as found in the present work, 7050-T7451 specimens did not fail when immersed in substitute ocean water at an applied stress of 400 MPa. Similarly, 7075-T73 plate material was susceptible to transgranular SCC in an aqueous NaCl solution with nitrate additions, but not in chloride environments containing sulfate and hydrogen carbonate, as demonstrated by constant load tests applying an initial stress of 300 MPa in short-transverse direction.[29] The environment-induced degradation might be associated with an enhanced localized corrosion attack caused by intergranular corrosion which was found to be promoted by nitrate added to chloride solutions.[53,54] This assumption is supported by a thorough fractographic examination of short-transverse tensile specimens of 7050-T7451 plate which were slow strain rate tested in aerated

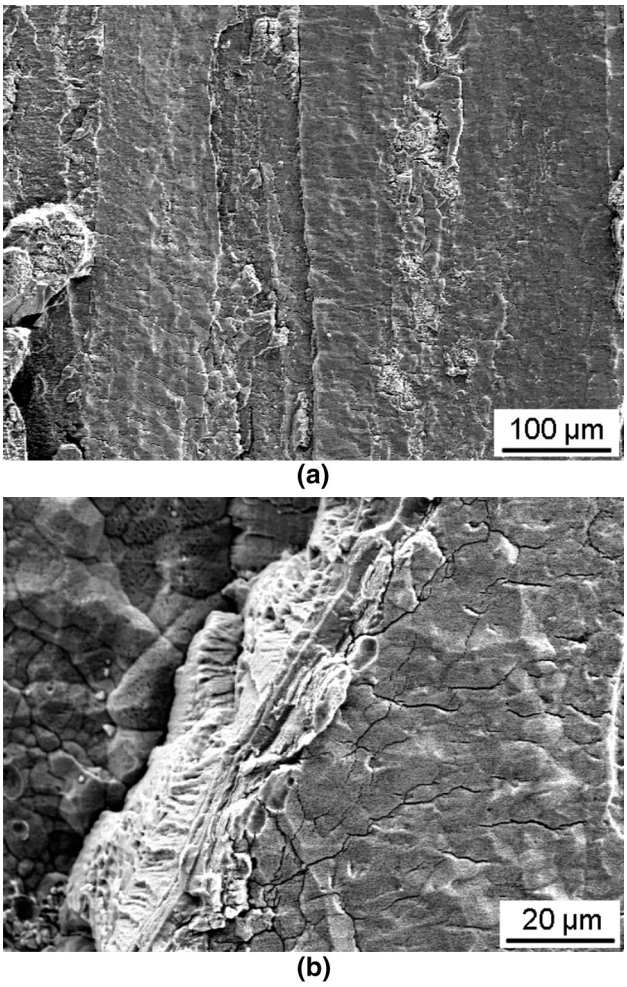

Fig. 9—Scanning electron micrographs of alloy 7050-T7451 showing (*a*) intergranular SCC and (*b*) transition between two intergranular fracture planes. The notched sample was cyclically loaded in substitute ocean water at a nominal frequency of 3.61×10^{-5} s^{-1}, applying a stress range $\Delta\sigma = 270$ MPa with $\sigma_{max} = 300$ MPa.

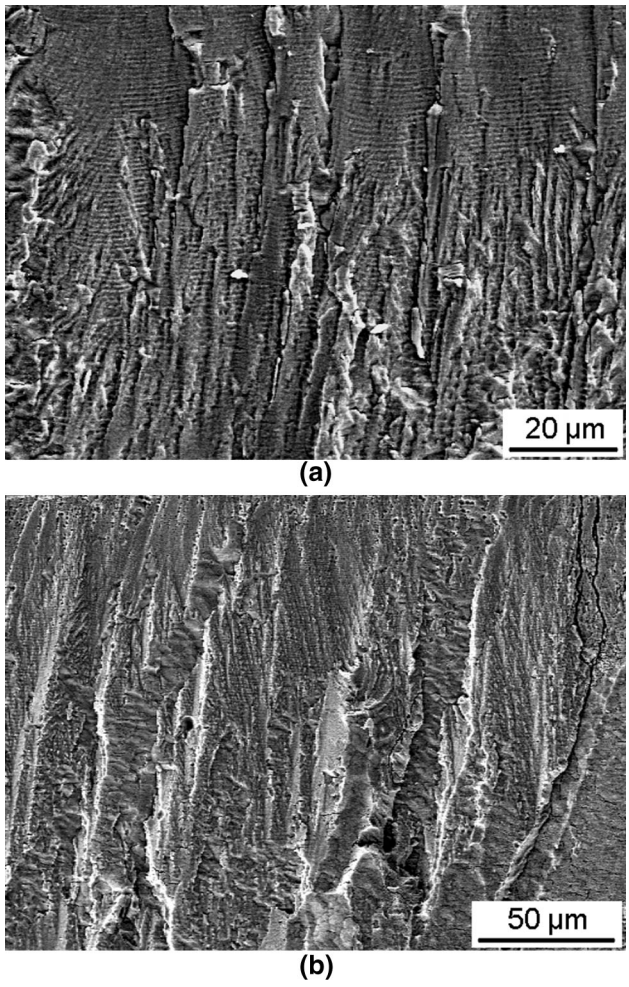

Fig. 10—Scanning electron micrographs of alloy 7050-T7451 showing cleavage-like fracture. The notched specimens were cyclically loaded in substitute ocean water at nominal frequencies of (*a*) 1.10×10^{-4} and (*b*) 1.91×10^{-4} s^{-1}, applying a stress range $\Delta\sigma = 270$ MPa with $\sigma_{max} = 300$ MPa.

3.5 pct NaCl solution.[13] The transgranular stress corrosion cracks propagating by a local discontinuous cleavage-like fracture were found to be associated with critical defects formed by localized dissolution. Therefore, the spots of transgranular SCC observed for 7050-T7451 specimens dynamically strained in substitute ocean water (Figure 3) were likely associated with pits promoted by this synthetic environment, as also found for 7050 plate in the tempers T7651 and T7351 exposed to the same corrosive medium.[41]

Several mechanisms have been proposed to explain transgranular stress corrosion crack propagation. They include film-induced cleavage,[55] hydrogen-enhanced decohesion (HEDE),[56,57] hydrogen-enhanced localized plasticity (HELP),[58,59] adsorption-induced dislocation emission (AIDE),[44,60] and corrosion-enhanced plasticity.[45,61] The description of these mechanisms is outside the scope of this paper; for more information, it is referred to the respective references. However, it is very difficult to identify by experimental results the mechanism being operative in transgranular environment-induced cracking in aluminum alloys. In most of the papers on transgranular SCC, hydrogen is considered to play an important role. Hydrogen in solid solution has been shown to inhibit cross-slip in high purity aluminum, thus promoting slip planarity.[62] This can result in a change of the ductile transgranular fracture into transgranular cleavage and brittle intergranular fracture mode. Such transitions to brittle transgranular/intergranular fracture were observed at the rim of the fracture surfaces of cathodically pre-charged tensile specimens of high purity 7075 alloy.[63] The embrittlement was associated with the effect of the matrix precipitates on the slip planarity, aggravated by coarse planar slip probably due to an enhanced hydrogen transport by dislocations. The transport of large amounts of hydrogen by dislocations into the material was demonstrated by cathodic charging of 7075 tensile specimens simultaneously strained in the plastic region at a slow strain rate.[64] This procedure resulted in the occurrence of pronounced intergranular fracture followed by a transgranular brittle region between the intergranular and the ductile overload

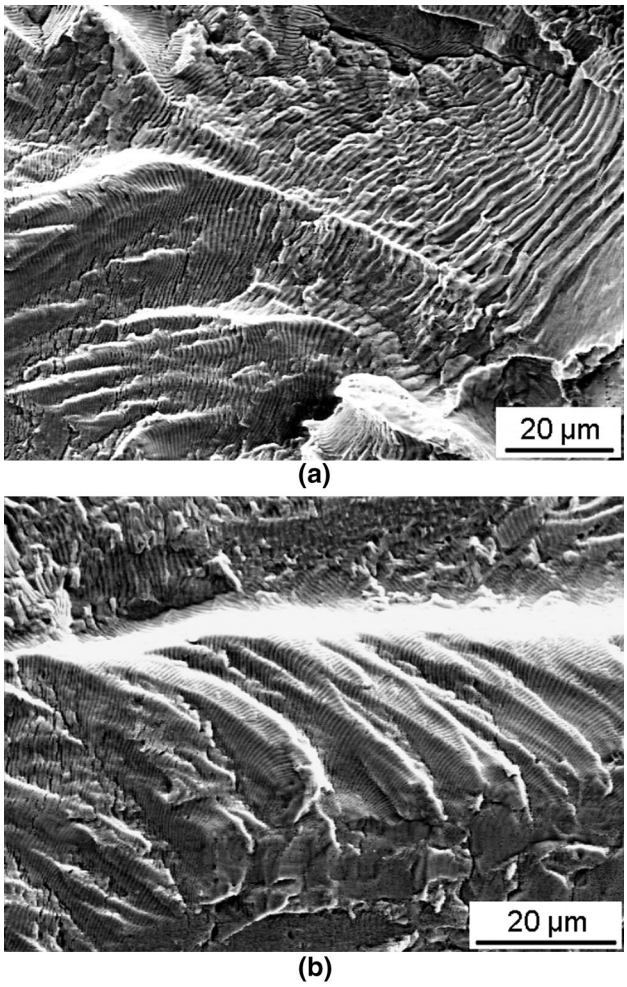

Fig. 11—Scanning electron micrographs of alloy 7050-T7451 showing striations crossing different cleavage-like facets. The notched sample was cyclically loaded in substitute ocean water at a nominal frequency of 6.40×10^{-4} s^{-1}, applying a stress range $\Delta\sigma = 270$ MPa with $\sigma_{max} = 300$ MPa.

fracture areas. The embrittlement by hydrogen was even more severe in the presence of notches. Apparently, embrittlement requires stress concentration with the embrittling species accumulating at or near the notches, resulting in microcrack formation within their plastic zone.[65]

Similarly, environmentally assisted fatigue cracking of high-strength aluminum alloys has mainly been associated with hydrogen embrittlement.[23,35,37,66–69] Thus, the deterioration in fatigue strength of alloy 7075-T6 caused by exposure to aqueous chloride and sulfate solutions was aggravated when corrosion fatigue testing was carried out under cathodic charging conditions.[35] On the fracture surfaces, pronounced cleavage and quasi cleavage were observed. A hydrogen embrittlement mechanism for corrosion fatigue cracking in peak-aged and overaged alloys 7050 and 7075 was also inferred from fractographic examinations which revealed cleavage cracking with fan-like pattern as well as brittle striations on specimens low- and high-cycle fatigue tested in chloride-containing aqueous solutions.[68,69] Similar results were obtained from fatigue tests of 7150-T651 plate material using compact tension specimens in S-L orientation.[23] When tests were performed in air, the crack growth rate did not depend on the applied frequencies ranging from 0.1 to 20 Hz; a mainly ductile transgranular fracture was observed. In an aqueous chromate-inhibited chloride solution, the corrosion fatigue crack growth rates were enhanced in comparison to those measured in air and they were dependent upon frequency, increasing with decreasing frequency. The crack propagation changed to brittle intergranular as well as brittle flat transgranular and crystallographic transgranular failure modes. Brittle intergranular fracture was prevailing at low ΔK and low frequency. A hydrogen embrittlement mechanism was proposed to operate in both intergranular and transgranular corrosion fatigue crack growth, involving grain boundary diffusion and dislocation transport of hydrogen, respectively, ahead of the crack tip.

Results obtained in the present work are in agreement with these studies on fatigue testing of high-strength aluminum alloys reported above. At very low frequencies, intergranular environment-induced cracking was observed, possibly indicating a remaining intergranular SCC sensitivity of alloy 7050 in the T7451 temper at applied stresses in short-transverse direction. Although not observed under static loading conditions, intergranular stress corrosion cracking might be promoted by cyclic loading inducing SCC below the threshold stress determined in static loading tests. Striations on the intergranular fracture planes indicated discontinuous crack propagation. Discontinuous intergranular stress corrosion crack propagation was also proposed for alloy 7075-T651, as corroborated by acoustic emission results and fractographic examinations revealing striation-like markings on the intergranular facets.[70] Whereas intergranular environmentally assisted cracking can be mitigated by overaging, this heat treatment has no effect on transgranular fracture.[35] Thus, the corrosion fatigue behavior of 7075 alloy was not improved by aging to the T73 temper which provides immunity to intergranular SCC.[35,68] Similarly, transgranular environmentally assisted cracking of 7050 plate material under cyclic loading conditions at low frequencies was not affected by applying different aging treatments.[15,52]

In the present cyclic loading tests of 7050-T7451 plate, the number of cycles-to-failure was found to be dependent on the square root of frequency (Figure 4(b)). This indicated an embrittlement mechanism controlled by diffusion, probably by hydrogen diffusion to the region ahead of the crack tip. At applied initial maximum stresses of both 300 and 400 MPa, no deviation in the slope of the cycles-to-failure *vs* frequency curves on a log-log basis was observed, as expected for a change from intergranular to transgranular fracture mode associated with different operating mechanisms. Therefore, both intergranular and transgranular environmentally assisted cracking are supposed to be caused by hydrogen embrittlement. Performing corrosion fatigue tests of alloy 7017-T651 in seawater at different frequencies, similar frequency dependence was observed for the critical crack velocity at which fracture mode

transitions occurred between intergranular to flat transgranular fracture and flat transgranular to striated ductile transgranular fracture.[66] Because this velocity depended upon the square root of the cycle period, the environment-enhanced crack growth rate was attributed to hydrogen diffusion ahead of the crack tip. Recently, a hydrogen-environment embrittlement mechanism has been favored for environmental fatigue crack growth in aluminum, causing a localized reduction of the cohesive strength of the material.[71,72] Such a mechanism is also proposed to be operative in the environmentally assisted cracking in alloy 7050-T7451 under cyclic loading at very low frequencies.

V. CONCLUSIONS

The environment-induced cracking behavior of 7050-T7451 plate material was investigated under constant load, constant extension rate, and cyclic loading conditions using short-transverse smooth and notched tensile specimens which were permanently immersed in substitute ocean water and an aqueous solution of 0.6 M NaCl + 0.06 M $(NH_4)_2SO_4$. The following results were obtained:

1. The alloy was immune to stress corrosion cracking under static loading condition. No failure occurred in both synthetic environments at an applied stress of 400 MPa.
2. High SCC resistance was also found performing constant extension rate tests. The corrosive environments did not deteriorate the fracture energy and notch strength of dynamically strained samples.
3. Notched tensile specimens failed predominantly by transgranular environment-induced cracking when cyclically loaded in substitute ocean water applying displacement rates ranging from 2×10^{-6} to 2×10^{-4} mms^{-1}.
4. At a given displacement rate, the time-to-failure was shorter at higher applied maximum stress. The number of cycles-to-failure decreased with decreasing nominal frequency.
5. Plots of the number of cycles-to-failure *vs* nominal frequency curves on a log-log basis revealed a linear dependence. A slope of about 0.5 was obtained by linear fitting, supporting a diffusion-controlled degradation mechanism, most likely hydrogen embrittlement.
6. Striations on the brittle fracture surfaces indicated discontinuous crack propagation.

REFERENCES

1. D.O. Sprowls and R.H. Brown: in *Fundamental Aspects of Stress Corrosion Cracking*, R.W. Staehle, ed., National Association of Corrosion Engineers, Houston, 1969, pp. 466–506.
2. M.O. Speidel: *Metall. Trans. A*, 1975, vol. 6A, pp. 631–51.
3. T.J. Summerson and D.O. Sprowls: in *Aluminum Alloys - Their Physical and Mechanical Properties*, E.A. Starke and T.H. Sanders, eds., EMAS, Cradley Heath, 1986, pp. 1575–662.
4. N.J.H. Holroyd: in *Environment-Induced Cracking of Metals*, R.P. Gangloff and M.B. Ives, eds., National Association of Corrosion Engineers, Houston, 1990, pp. 311–45.
5. W.H. Hunt and J.T. Staley: in *Light-Weight Alloys for Aerospace Applications*, E.W. Lee, E.H. Chia, and N.J. Kim, eds., The Minerals, Metals & Materials Society, Warrendale, 1989, pp. 111–20.
6. R.J. Bucci, C.J. Warren, and E.A. Starke: *J. Aircraft*, 2000, vol. 37, pp. 122–29.
7. E.A. Starke and J.T. Staley: *Prog. Aerospace Sci.*, 1996, vol. 32, pp. 131–72.
8. N.J.H. Holroyd, A.K. Vasudevan, and L. Christodoulou: in *Aluminum Alloys—Contemporary Research and Applications,* A.K. Vasudevan and R.D. Doherty, eds., Treatise on Materials Science and Technology, Vol. 31, Academic Press, Boston, 1989, pp. 463–83.
9. M.C. Reboul, T. Magnin, and T.J. Warner: in *Aluminium Alloys – Their Physical and Mechanical Properties (ICAA3), Vol. II*, L. Arnberg, O. Lohne, E. Nes, and N. Ryum, eds., NTH and SINTEF, Trondheim, 1992, pp. 453–60.
10. W. Gruhl: *Z. Metallkde.*, 1984, vol. 75, pp. 819–26.
11. T.D. Burleigh: *Corrosion*, 1991, vol. 47, pp. 89–98.
12. M.C. Reboul and B. Baroux: *Mater. Corros.*, 2010, vol. 61, No. 9999.
13. D. Najjar, T. Magnin, and T.J. Warner: *Mater. Sci. Eng. A*, 1997, vol. 238, pp. 293–302.
14. R. Braun: *Materialwiss. Werkstofftech.*, 2007, vol. 38, pp. 674–89.
15. R. Braun: *Int. J. Fatigue*, 2008, vol. 30, pp. 1827–37.
16. R. Braun: in *Effects of Hydrogen on Materials*, B. Somerday, P. Sofronis, and R. Jones, eds., ASM International, Materials Park, 2009, pp. 251–58.
17. R.H. Jones and R.E. Ricker: in *Stress-Corrosion Cracking*, R.H. Jones, ed., ASM International, Materials Park, 1992, pp. 1–40.
18. D.O. Sprowls: in *Stress-Corrosion Cracking*, R.H. Jones, ed., ASM International, Materials Park, 1992, pp. 363–415.
19. P.S. Pao, R.A. Bayles, S.J. Gill, D.A. Meyn, and G.R. Yoder: in *Parkins Symposium on Fundamental Aspects of Stress Corrosion Cracking*, S.M. Bruemmer, E.I. Meletis, R.H. Jones, W.W. Gerberich, F.P. Ford, and R.W. Staehle, eds., TMS, Warrendale, 1992, pp. 245–54.
20. P.S. Pao, S.J. Gill, R.A. Bayles, and G.R. Yoder: *Scripta Met.*, 1991, vol. 25, pp. 2085–89.
21. R.N. Parkins and B.S. Greenwell: *Metal Sci.*, 1977, vol. 11, pp. 405–13.
22. D. Wu, H.S. Ahluwalia, H. Cai, J.T. Evans, and R.N. Parkins: *Corros. Sci.*, 1991, vol. 32, pp. 769–94.
23. A.D.B. Gingell and J.E. King: *Acta Mater.*, 1997, vol. 45, pp. 3855–70.
24. Z.M. Gasem and R.P. Gangloff: *Mater. Sci. Forum*, 2000, vols. 331–337, pp. 1479–88.
25. S.B. Lyon, G.E. Thompson, and J.B. Johnson: in *New Methods for Corrosion Testing of Aluminum Alloys, ASTM STP 1134*, V.S. Agarwala and G.M. Ugiansky, eds., American Society for Testing and Materials, Philadelphia, 1992, pp. 20–31.
26. T.E. Graedel: *J. Electrochem. Soc.*, 1989, vol. 136, pp. 204C–12C.
27. A.H. Le, B.F. Brown, and R.T. Foley: *Corrosion*, 1980, vol. 36, pp. 673–9.
28. R. Braun: *Mater. Corros.*, 2000, vol. 51, pp. 607–15.
29. R. Braun: *Mater. Corros.*, 2003, vol. 54, pp. 157–62.
30. R. Braun: *Mater. Corros.*, 2004, vol. 55, pp. 241–48.
31. R. Braun and H. Buhl: in *Advanced Aerospace Materials*, H. Buhl, ed., Springer, Berlin, 1992, pp. 296–307.
32. C.R. Hutchinson, F. de Geuser, Y. Chen, and A. Deschamps: *Acta Mater.*, 2014, vol. 74, pp. 96–109.
33. R.E. Stoltz and R.M. Pelloux: *Corrosion*, 1973, vol. 29, pp. 13–7.
34. M. Khobaib, C.T. Lynch, and F.W. Vahldiek: *Corrosion*, 1981, vol. 36, pp. 285–92.
35. R.J. Jacko and D.J. Duquette: *Metall. Trans. A*, 1977, vol. 8A, pp. 1821–27.
36. R.E. Stoltz and R.M. Pelloux: *Metall. Trans. A*, 1972, vol. 3A, pp. 2433–41.
37. J. Ruiz and M. Elices: *Corros. Sci.*, 1996, vol. 38, pp. 1815–37.
38. M. Puiggali, A. Zielinsky, J.M. Olive, E. Renauld, D. Desjardins, and M. Cid: *Corros. Sci.*, 1998, vol. 40, pp. 805–19.
39. R. Braun: *Mater. Corros.*, 1993, vol. 44, pp. 73–82.

40. R. Braun: *Mater. Corros.*, 1994, vol. 45, pp. 369–77.
41. R. Braun: *Corrosion*, 1997, vol. 53, pp. 467–74.
42. E.N. Pugh: *Corrosion*, 1985, vol. 41, pp. 517–26.
43. M.J. Kaufman and J.L. Fink: *Acta Metall.*, 1988, vol. 36, pp. 2213–28.
44. S.P. Lynch: *Acta Metall.*, 1988, vol. 36, pp. 2639–61.
45. T. Magnin, A. Chambreuil, and J.P. Chateau: *Int. J. Fracture*, 1996, vol. 79, pp. 147–63.
46. J.L. Nelson and E.N. Pugh: *Metall. Trans. A*, 1975, vol. 6A, pp. 1459–60.
47. R.C. Dorward and K.R. Hasse: *Corros. Sci.*, 1982, vol. 22, pp. 251–57.
48. R. Braun: *Mater. Corros.*, 1994, vol. 45, pp. 255–63.
49. R. Braun: *Mater. Corros.*, 2005, vol. 56, pp. 159–65.
50. R. Braun: *Mater. Charact.*, 2006, vol. 56, pp. 85–95.
51. R. Braun: in *Corrosion-Deformation Interactions CDI '96*, T. Magnin, ed., The Institute of Materials, London, 1997, pp. 140–47.
52. R. Braun: in *Hydrogen Effects on Material Behavior and Corrosion Deformation Interactions*, N.R. Moody, A.W. Thompson, R.E. Ricker, G.W. Was, and R.H. Jones, eds., TMS, Warrendale, 2003, pp. 883–92.
53. S. Maitra and G.C. English: *Metall. Trans. A*, 1982, vol. 13A, pp. 161–66.
54. J.F. McIntyre and T.S. Dow: *Corrosion*, 1992, vol. 48, pp. 309–19.
55. K. Sieradzki and R.C. Newman: *Philos. Mag. A*, 1985, vol. 51, pp. 95–132.
56. R.A. Oriani: *Corrosion*, 1987, vol. 43, pp. 390–97.
57. R.A. Oriani: in *Environment-Induced Cracking of Metals*, R.P. Gangloff and M.B. Ives, eds., National Association of Corrosion Engineers, Houston, 1990, pp. 439–48.
58. H.K. Birnbaum and P. Sofronis: *Mater. Sci. Eng. A*, 1994, vol. 176, pp. 191–202.
59. H.K. Birnbaum, I.M. Robertson, P. Sofronis, and D. Teter: in *Corrosion-Deformation Interactions CDI '96*, T. Magnin, ed., The Institute of Materials, London, 1997, pp. 172–95.
60. S.P. Lynch: in *Corrosion-Deformation Interactions CDI '96*, T. Magnin, ed., The Institute of Materials, London, 1997, pp. 206–19.
61. D. Delafosse and T. Magnin: *Eng. Fract. Mech.*, 2001, vol. 68, pp. 693–729.
62. P.J. Ferreira, I.M. Robertson, and H.K. Birnbaum: *Acta Mater.*, 1999, vol. 47, pp. 2991–98.
63. D. Nguyen, A.W. Thompson, and I.M. Bernstein: *Acta Metall.*, 1987, vol. 35, pp. 2417–25.
64. J. Albrecht, I.M. Bernstein, and A.W. Thompson: *Metall. Trans. A*, 1982, vol. 13A, pp. 811–20.
65. K. Sadananda and A.K. Vasudevan: *Metall. Mater. Trans. A*, 2011, vol. 42A, pp. 279–95.
66. N.J.H. Holroyd and D. Hardie: *Corros. Sci.*, 1983, vol. 23, pp. 527–46.
67. R.E. Ricker and D.J. Duquette: *Metall. Trans. A*, 1988, vol. 19A, pp. 1775–83.
68. C.-K. Lin and S.-T. Yang: *Eng. Fract. Mech.*, 1998, vol. 59, pp. 779–95.
69. E.U. Lee, A.K. Vasudevan, and G. Glinka: *Int. J. Fatigue*, 2009, vol. 31, pp. 1938–42.
70. P. Martin, J.I. Dickson, and J.-P. Bailon: *Mater. Sci. Eng.*, 1985, vol. 69, pp. L9–L13.
71. R.P. Gangloff: in *Comprehensive Structural Integrity, Vol. 6*, I. Milne, R.O. Ritchie and B. Karihaloo, eds., Elsevier Science, New York, 2003, pp. 31–101.
72. Y. Ro, S.R. Agnew, and R.P. Gangloff: *Metall. Mater. Trans. A*, 2008, vol. 39A, pp. 1449–65.